Science of the Total Environment 855 (2023) 158924

Contents lists available at ScienceDirect

Science of the Total Environment

journal homepage: www.elsevier.com/locate/scitotenv

Dose–response mapping of MEHP exposure with metabolic changes of trophoblast cell and determination of sensitive markers

Yiwei Fang [a,1], Zhiliang Chen [b,1], Jinyu Chen [a,1], Minqi Zhou [a], Yuanyao Chen [a], Rong Cao [a], Chunyan Liu [a], Kai Zhao [a], Min Wang [b,*], Huiping Zhang [a,*]

[a] Institute of Reproductive Health, Tongji Medical College, Huazhong University of Science and Technology, Wuhan 430030, PR China
[b] Wuhan Prevention and Treatment Center for Occupational Diseases, Wuhan 430015, PR China

HIGHLIGHTS

- Higher doses of MEHP lead to stronger metabolic perturbations in trophoblast cells.
- Amino acid, pyrimidine, and glutathione metabolism were affected by MEHP.
- 5′-UMP and *N*-acetylputrescine as potential sensitively markers for MEHP exposure.

GRAPHICAL ABSTRACT

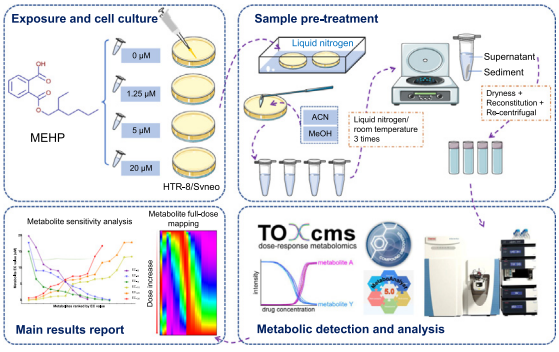

ARTICLE INFO

Editor: Lidia Minguez Alarcon

Keywords:
Mono(2-ethylhexyl) phthalate
Metabolomics
Exposure
Biomarker
Adverse pregnancy outcomes

ABSTRACT

Mono(2-ethylhexyl) phthalate (MEHP) is a metabolite of DEHP which is one of phthalic acid esters (PAEs) widely used in daily necessities. Moreover, MEHP has been proven to have stronger biological toxicity comparing to DEHP. In particular, several recent population-based studies have reported that intrauterine exposure to MEHP results in adverse pregnancy outcomes. To explore the mechanisms and metabolic biomarkers of MEHP exposure, we examined the metabolic status of HTR-8/Svneo cell lines exposed to different doses of MEHP (0, 1.25, 5.0, 20 μM). Global and dose–response metabolomics tools were used to identify metabolic perturbations and sensitive markers associated with MEHP. Only 22 metabolic features (accounted for <1 %) were significantly changed when exposed to 1.25 μM. However, when the exposure dose was increased to 5 or 20 μM, the number of significantly changed metabolic features exceeded 300 (approximately 10 %). In particular, amino acid metabolism, pyrimidine metabolism and glutathione metabolism were widely affected according to the enrich analysis of those significant altered metabolites, which has and have previously been reported to be closely related to fetal development. Moreover, 5′-UMP and *N*-acetylputrescine with the lowest effective concentrations (EC_{-10} = 0.1 μM and EC_{+10} = 0.11 μM, respectively) were identified as sensitive endogenous biomarkers of MEHP exposure.

1. Introduction

As a class of lipophilic chemicals, phthalic acid esters (PAEs) are widely used as common plasticizers added to polymeric materials to improve their flexibility and workability (Elimam et al., 2017). With a wide range of great

* Corresponding authors.
E-mail addresses: 14967955@qq.com (M. Wang), zhpmed@126.com (H. Zhang).
[1] These authors have contributed equally to this work.

http://dx.doi.org/10.1016/j.scitotenv.2022.158924
Received 4 August 2022; Received in revised form 18 September 2022; Accepted 18 September 2022
Available online 22 September 2022

characteristic properties including good insulation, high strength, excellent corrosion resistance, low cost, and ease of fabrication, PAEs are broadly used in numerous consumer products, for instance, cosmetics, food packaging, building materials, medical supplies, and home furnishings. (Chi et al., 2017; He et al., 2019). During recent decades, global industrialization has massively increased plastic production, raising the use of additives such as PAEs. The global production of PAEs in 2018 was estimated at 300 million tons, and it is expected to reach 500 million tons by 2050, most of which will be single-use products (Sardon and Dove, 2018). The extensive application of PAEs has attracted increasing attention as environmental and biomedical pollutants, which may invisibly enter the human body through airborne transmission, skin contact, and contaminated food and drink, constituting potential health threats (Gani et al., 2017).

Di(2-ethylhexyl) phthalate (DEHP), one of the PAEs more widely distributed in the environment, has been broadly proven to adversely impact health. Mono(2-ethylhexyl) phthalate (MEHP) is a bioactive metabolite of DEHP, which is also hazardous to health (Hanioka et al., 2017). Furthermore, MEHP was found in a variety of body fluids, including blood, urine, semen, and breast milk (Martinez-Razo et al., 2021). It has been proven to be toxic to the liver (Doull et al., 1999; Xu et al., 2022), kidneys (Liu et al., 2022) and metabolism (Minguez-Alarcon et al., 2022; Wei et al., 2022). In addition, MEHP was found to be highly toxic to reproduction. MEHP could act through a receptor-mediated signaling pathway to inhibit the production of estradiol, interfere with the modulation of the hypothalamic-pituitary-ovarian axis, suppress the synthesis of sex hormones, and cause sex hormone secretion disorders, resulting in severe toxicity in the female reproductive system (Li et al., 2020). More importantly, MEHP impaired testicular development in embryonic mice by inducing oxidative stress (Zhang et al., 2020b).

MEHP can pass through the placenta and result in adverse birth outcomes including miscarriage (Aimuzi et al., 2022; Martinez-Razo et al., 2021). A large case–control study from China showed that unexplained recurrent spontaneous abortion was associated with higher concentrations of MEHP (Aimuzi et al., 2022). It is worth noting that MEHP exposure during pregnancy significantly impairs fetal development. Recently, several studies have suggested that DEHP/MEHP negatively impacts placental physiological processes such as trophoblast differentiation, invasion, endocrine function, and the oxidative stress response, which may lead to adverse pregnancy outcomes (Midic et al., 2018; Perez-Albaladejo et al., 2017; Zhang et al., 2020a). The placenta, as a medium for the exchange of maternal and fetal nutrients and metabolic wastes, begins its development when the blastocyst outer layer, the trophectoderm, adheres to the endometrium. Once adhered, trophectoderm cells that are considered trophoblast stem cells differentiate into cytotrophoblasts, which initiate the invasion process and then differentiate into either syncytiotrophoblasts or extravillous cytotrophoblasts (James et al., 2012; Pollheimer et al., 2018). The normal growth and differentiation of trophoblast cells is very important for placental development. MEHP affects many functions of trophoblast cells and thus placental function. Luis et al. proposed that the effects of MEHP on the placenta are mainly focused on implantation, differentiation, invasion, angiogenesis, oxidative stress response, metabolism, transfer of nutrients, hormonal signaling, immunomodulation and inflammatory response (Martinez-Razo et al., 2021). HTR-8/Svneo is an extravillous trophoblast cell line that can be used as an ideal in vitro model for studying the reproductive toxicity of MEHP (Abou-Kheir et al., 2017). HTR-8/Svneo cells with functions of proliferation and invasion, were separated from the placenta that is the target organ of MEHP. Moreover, some studies have shown that MEHP exposure might seriously affect the lipid metabolism process of trophoblast cells (Xu et al., 2005, 2006). However, other important metabolic processes and nonpolar metabolites have not received sufficient attention. For example, it is unknown whether MEHP affects the amino acid metabolism pathway which has been proven to be very important for the development of the fetus.

MEHP causes great harm to fetal development, and it is extremely urgent to establish an effective method to reflect MEHP exposure. However, existing direct tests for MEHP are time-consuming, laborious and costly, which greatly limit the early detection of MEHP. Importantly, the development of metabolomics seems to provide a new idea for the detection of MEHP. With advancements in omics-based technologies, metabolomics, a high-throughput analytical platform capable of quantifying a large number of metabolites from exogenous and endogenous sources, has emerged as a powerful tool to improve internal biological effects and metabolic perturbation estimations in complex environmental exposure (Liang et al., 2018). Recently, Yao et al. developed a software called TOXcms for dose–response metabolomics to understand biochemical mechanisms and off-target drug effects (Yao et al., 2020). This approach with unique advantages can be used to explore highly sensitive metabolic markers of pollutant exposure (Zhao et al., 2022). However, there is currently no metabolite to accurately and sensitively determine MEHP exposure.

From the above, it is of great practical significance to judge the exposure level of MEHP through the sensitive change in metabolites. To address this gap, we performed an untargeted metabolomic analysis and identified a dose–response profile of MEHP exposure in the HTR-8/SVneo cell line, hoping to explore sensitive and accurate metabolites for determining the event of MEHP exposure.

2. Materials and methods

2.1. Cell culture and MEHP treatment

The HTR-8/SVneo cell line was purchased from Shanghai Suer Biotechnology Co., Ltd. (China) and maintained in RPMI-1640 (Gibco, USA) with 10 % fetal bovine serum (Gibco, USA). The cells were cultured at 5 % CO_2, 95 % humidity, and 37 °C. MEHP for treating cells was purchased from Aladdin (China), and dimethyl sulfoxide (DMSO, Beijing SolarbioScience & TechnologyCo., Ltd., China) was used to prepare the single-compound stock solution. The dose group consisted of either a vehicle control group containing 0.1 % DMSO (0 μM) or 1.25 μM, 5 μM, or 20 μM MEHP exposure groups, all exposed for 24 h.

2.2. Metabolite extraction

2.2.1. Cell quenching

After 24 h of cell exposure, the cell dish was removed from the incubator, placing it on ice, discarding the medium in the dish, rinsing with PBS and repeating three times, and draining the dish. Then, the culture dish was placed in a container containing liquid nitrogen to quench the cells.

2.2.2. Cell sample pretreatment

Sample pretreatment was performed according to Beyer et al. (2018) with some modifications. Specifically, precooled methanol (MeOH): acetonitrile (ACN) (1:1, *v*/v) was added to the cell culture dish, scraping the cells with a cell scraper, transferring the cell suspension to the centrifuge tube, adding an appropriate amount of MeOH/ACN (1:1, *v*/v) solution to clean the remaining cells in the cell culture dish, and transferring it to the same centrifuge tube. The above processes were performed on ice. Then, centrifuge tubes were placed into liquid nitrogen/room temperature circulating freeze–thaw cycles three times, vortexed for 3 min to mix the sample, and centrifuged for 15 min (13,000 rpm, 4 °C). The supernatant was transferred to new centrifuge tubes and evaporated with a vacuum centrifugal concentrator. The metabolic extract was redissolved with H_2O/ACN (95:5, *v*/v), vortexed for 5 min, and centrifuged again. Ten microliters of supernatant from each of the 24 tube samples was mixed as a quality control (QC) sample, and the remaining supernatant was transferred to glass injection bottles for subsequent liquid chromatography-mass spectrometry (LC-MS) analysis.

2.3. LC–MS analysis and data processing

The supernatant was analyzed by UPLC-Q-Exactive-MS/MS (Thermo Fisher Scientific, USA). Details of the profiling method were modified based on Shen et al. (2021) and Chen et al. (2022). Details of LC–MS

analysis and data processing can be found in the Supplementary Information. Briefly, QC analysis was performed every 10 injections of biological samples and blank samples (H_2O: ACN, 95:5, *v*/v) after setting the parameters of the device. Full scan mode was used to collect first-order mass spectrum information, and data-dependent acquisition (DDA) mode was used to collect second-order mass spectrum information from QC samples. We used Compound Discoverer (CD, version 3.1) for peak alignment and annotations.

2.4. Metabolic profiling and pathway analysis

MetaboAnalyst 5.0 (Pang et al., 2021), a user-friendly and streamlined metabolomics data analysis software, has been used in most metabolomics studies. Before further analysis, metabolic intensities were log2-transformed and autoscaling. MetaboAnalyst 5.0 and R software (version 4.1.2) were used to perform principal component analysis (PCA), heatmaps, volcano maps, and enrichment analysis. The significant features were screened with false discovery rate (FDR) ≤ 0.05, and fold change (FC) >1.1 or FC <0.9.

2.5. TOXcms metabolomics and perturbation biomarker screening

The TOXcms software was designed by Yao et al. to support dose–response metabolomics analysis (Yao et al., 2020). A fundamental principle of this software is to trace each of the metabolites detected in an untargeted metabolomics experiment through a series of related perturbations or exposures, such as an increasing dose of a drug or toxicant. TOXcms analyses each feature intensity plot as a function of perturbation or exposure, and then classifies each trend as increasing, decreasing, decreasing and increasing, or unchanging over the sample groups. The methods of perturbation biomarker screening refer to Zhao et al. (2022) Using the TOXcms R-package, we processed the metabolite profiling data in CSV format. We selected features with statistically significant dose–response relationships that were recognized by TOXcms for comparison with global metabolomics results and identification of off-target compounds. On the basis of the fold changes of the significantly dysregulated metabolites, a dose–response relationship was established, with dose levels ranging from 0 μM to 20 μM continuously. For each metabolite, the most appropriate dose–response fitting method was selected from a comprehensive set of regression models, which included linear, Hill, exponential, polynomial, and Gauss-probit models. Using these prediction models, we plotted metabolic dose mapping cartography and specific effective concentrations (ECs) were also calculated. Graphs were plotted using R software (version 4.1.2) and GraphPad Prism (version 9).

2.6. Statistical analysis

Six biological replicates were set up for each group, and each sample was detected once in pos mode and once in neg mode. When comparing metabolite changes in the exposure groups later, we pre-calculated the FC of metabolite levels through each sample relative to the control group (sample assay metabolite levels/mean metabolite levels of control samples). We analyzed the differences in metabolites between the three exposure groups and the control group using the one-way ANOVA. And $P < 0.05$ was considered statistically significant.

3. Results

3.1. Metabolomics profiling

In total, 3041 metabolic features were identified in the different samples (782 in the positive mode and 2259 in the negative mode) after quality control, data filtering, and normalization. By using PCA, the samples were distributed based on their first two components according to the dose of MEHP (Fig. 1A). The heatmap shows the relative level changes of all the global metabolic features in the four MEHP dose groups (Fig. 1B). When exposed to 1.25 μM MEHP, only 22 metabolic features (<1 %) were significantly changed. Moreover, when the concentration of MEHP increased to 5.0 μM, 327 metabolic features changed significantly (approximately 10 %), most of which were elevated. Even when MEHP concentrations were elevated to 20.0 μM, the number of dysregulated metabolic features was no longer altered, but the proportion of downregulated metabolic features among them slightly increased (Fig. 1C and D). All these results suggest that MEHP exposure at a dose of 1.25 μM has minimal metabolic disruption to trophoblasts, which becomes more pronounced as the exposure dose increases.

3.2. Dysregulated metabolite enrichment and identification

Moreover, we also paid particular attention to the metabolic state of the HTR-8/SVneo cell line at an exposure dose of 20.0 μM, including 263 upregulated and 64 downregulated metabolic features (Fig. 2A). After comparing the MS2 information with the mass spectrometry database, a total of 59 significantly dysregulated metabolites, mainly including amino acids and peptides, pyrimidines, and purines, were identified (Fig. 2B). These dysregulated metabolites were mainly enriched in amino acid metabolism, pyrimidine metabolism, and glutathione metabolism pathways (Fig. 2C). Alanine (a nonessential amino acid) and threonine (an essential amino acid) were both significantly downregulated (FC = 0.69 and 0.54, respectively) after 20.0 μM MEHP exposure. We also observed significant decreases in some antioxidants, such as vitamin C (FC = 0.72) and glutathione (FC = 0.08).

Overall, TOXcms screened 317 dysregulated metabolic features, including 242 metabolic characteristics with monotonically increasing or decreasing dose–response trends and 75 with reverse trends (Fig. 1D). Combined with global metabolomics and dose–response metabolomics, a total of 596 metabolic features were screened. Specifically, 279 (49.83 %) metabolic features were screened by global metabolomics only, 94 (15.77 %) by dose–response metabolomics only, and 223 (37.42 %) common metabolic features were screened by both (Fig. 1D). Based on the MS2 information, these metabolic features were accurately matched to 78 compounds. According to the Human Metabolome Database (HMDB) and Kyoto Encyclopedia of Genes and Genomes (KEGG) databases, the remaining 30 endogenous metabolites were used for subsequent analysis after excluding 48 exogenous metabolites (Table S1). The metabolite heatmap along with the bar graph is presented in Fig. 3 Most of the metabolites showed a monotonous trend, but some showed a reverse trend. For example, hexanoylcarnitine presented the lowest fold change (FC = 0.57) at 5.0 μM, while it recovered (FC = 0.94) at 20 μM within the applicable dose range.

3.3. Metabolite dose–response relationship characterization

We also determined the dose–response relationship and fitted dose–response curves for patterns of 30 dysregulated metabolites. Fig. 4 shows a complete dose map of all the identified metabolites within the scope of application, except for the three-metabolite (L-lactic acid, uridine diphosphate glucose (UDPAG), and decanoylcarnitine) dose–response relationships that were not well fitted. At the same time, Fig. 4 shows the dose–response curves of six representative metabolites that could be divided into three classes. Most models showed reasonable ascertainment coefficients and acceptable confidence coefficients, whereas several presented some degree of ambiguity in the 5–20 μM range and had greater confidence and prediction bands (e.g. hexanoylcarnitine). This is mainly due to few dose levels for high concentration areas.

3.4. Metabolite EC value calculation and perturbation biomarker screening

We sought to identify some special events to quantify effective important concentrations during metabolite changes. For continuous responses, a benchmark response is a predetermined response level, such as a 10 % increase from controls (Crizer et al., 2021). Therefore, two baseline

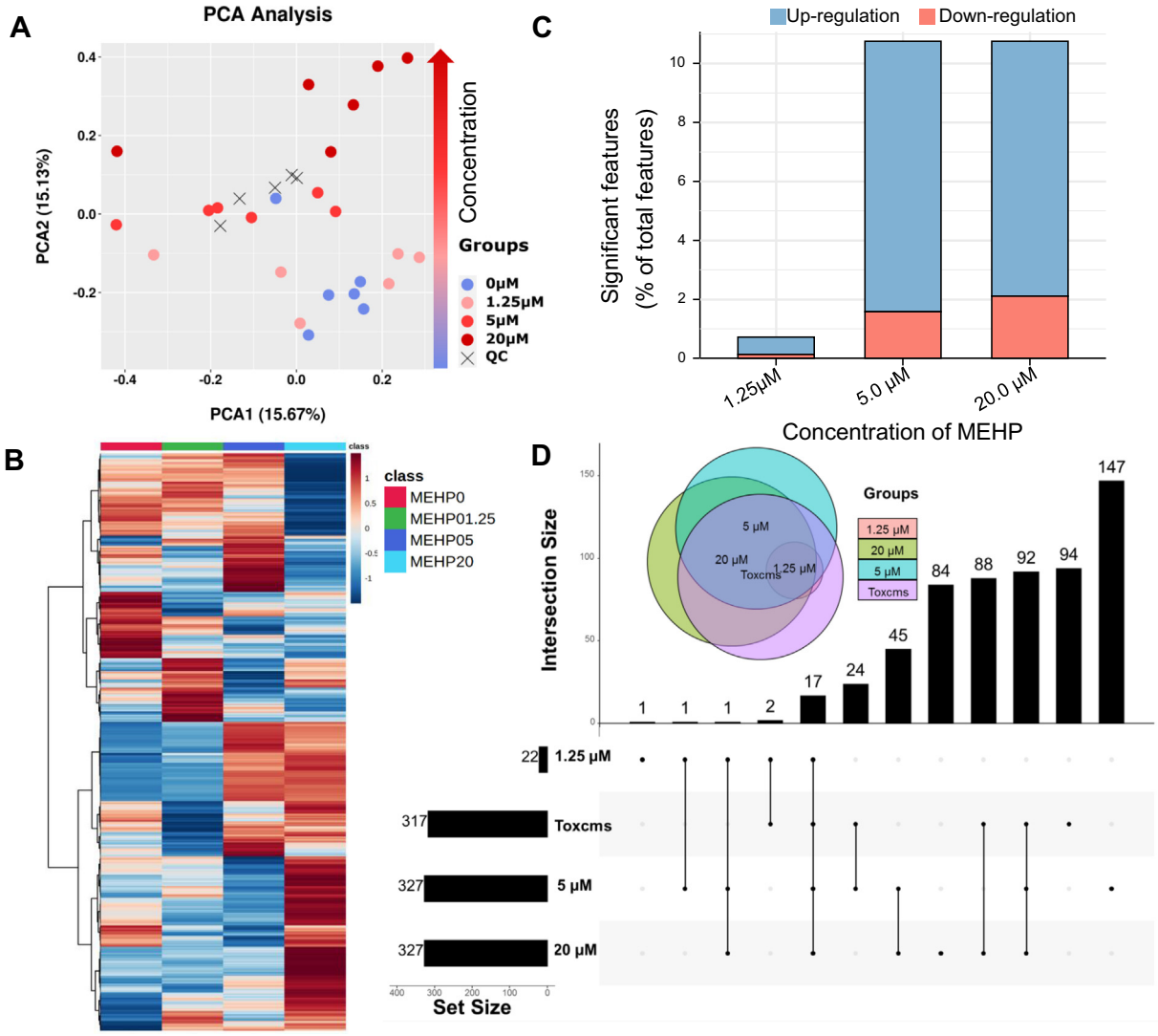

Fig. 1. Metabolomics profiling for all dose groups (0 μM, 1.25 μM, 5 μM, 20 μM). (A) Score plot of PCA based on HTR-8/SVneo cell metabolic profiling in the four dose groups. (B) Relative intensity of metabolites in the four dose groups. (C) The percentage of up- and down-regulated features detected using global profiling. (D) Upset diagram summarizing the number of shared and distinct dysregulated features of TOXcms and the global metabolome at 1.25 μM, 5 μM, and 20 μM.

indicators, 10 % downregulated EC (EC_{-10}) and 10 % upregulated EC (EC_{+10}), were first defined to provide information on the sensitivity of metabolite regulation to exposure stress (Table S2). To screen for more accurate and reliable MEHP exposure markers, we envisage additional indicators for assessment. With the pinpoint of EC_{+20}, EC_{+30}, EC_{-20}, EC_{-30}, higher fold changes of 20 % and 30 % were also introduced due to the uncertainties of metabolomics results (Table S2). Fig. 5 plots the sequence rankings of the six EC values for the 27 metabolites. In general, substances with lower EC values could serve as potential biomarkers of the metabolic perturbation effects of MEHP. We observed that uridine 5′-monophosphate (5′-UMP) was the metabolite with the lowest EC_{-10} (0.1 μM), while *N*-acetylputrescine showed the minimum EC_{+10} value (0.11 μM). For EC_{20} and EC_{30}, the metabolite sensitivity sequencing patterns were similar to that of EC_{10}, which indicates that the results of the prediction model are reliable.

4. Discussion

In this study, we performed an untargeted metabolomic analysis and identified a dose–response profile of MEHP exposure with metabolite changes in the HTR-8/SVneo cell line. Our results indicated that higher doses of MEHP lead to stronger metabolic perturbations in trophoblast cells. After continuous 24 h of exposure, the levels of some types of metabolites in cells changed significantly, such as amino acids, pyrimidines, and purines. Similarly, amino acid metabolism, pyrimidine metabolism, and glutathione metabolism pathways were also disrupted. Finally, we calculated EC values and identified 5′-UMP and *N*-acetylputrescine as potential markers for sensitively indicating MEHP exposure events.

Here, the dose of MEHP was carefully designed. Previous studies have reported MEHP concentrations ranging from 0.6 to 24.2 μM (median, 5.7 μM) in maternal peripheral blood and from 0.04 to 17.7 μM (median, 6.5 μM) in umbilical cord blood, suggesting that MEHP exposure levels are approximately equivalent in different body fluids (Li et al., 2013). In addition, Gao et al. found that HTR-8/SVneo cell viability was not significantly altered by MEHP exposure at concentrations ranging from 0 to 100 μM for 24 h (Gao et al., 2017). However, when the exposure time was extended to 72 h, the cell activity was significantly affected (Petit et al., 2018). Therefore, three dose groups (1.25 μM, 5 μM and 20 μM) were set and the exposure time was set at 24 h.

The results showed that the dysregulated metabolites might be highly correlated with the function of trophoblasts and the placenta. Among them, amino acids and its metabolic pathway disorders are particularly serious. Amino acids are essential nutrients for normal cell function, and a shortage of them has been shown to cause intrauterine growth restriction (Rosario et al., 2021). Although the body would be compensated in other

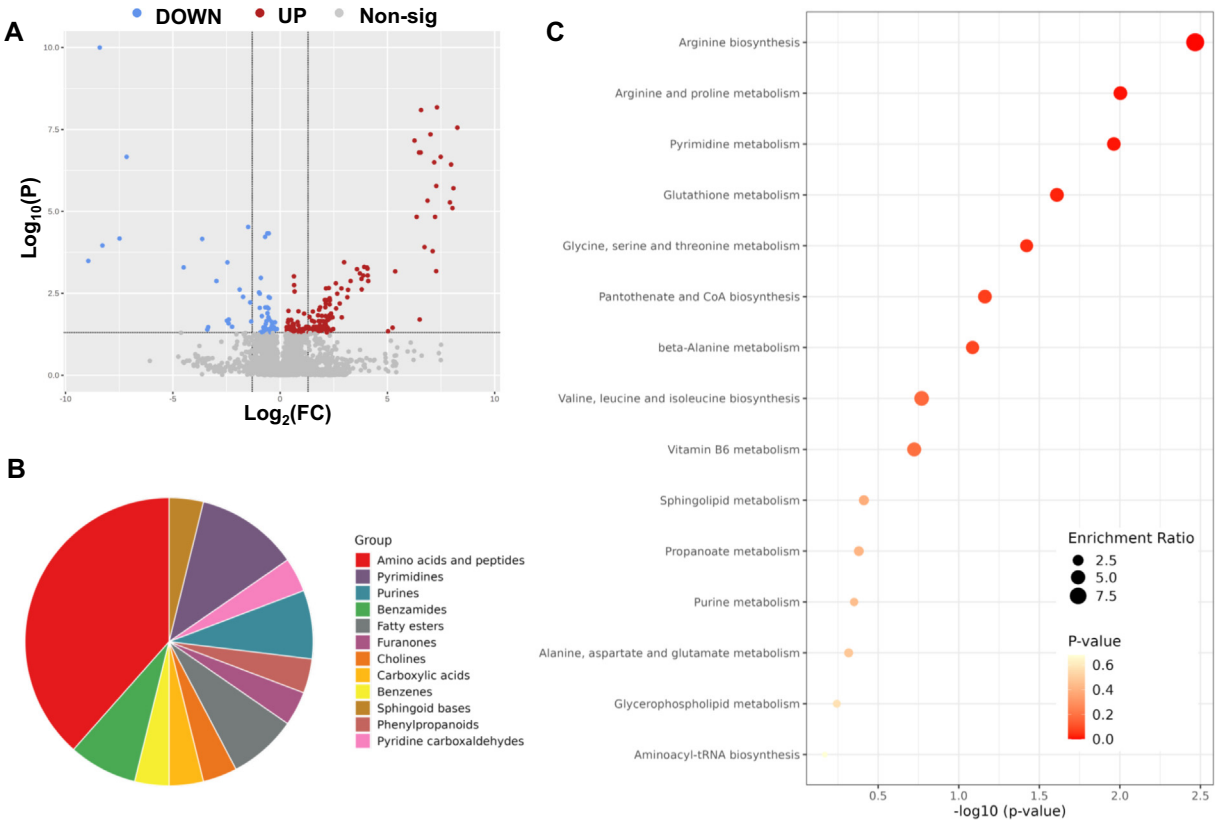

Fig. 2. Dysregulated metabolite enrichment in the 20 μM MEHP dose group. (A) The volcano map of up- and down-regulated metabolic features. (B) Pie chart of the main classes of identified metabolites. (C) Metabolite enrichment analysis of cells exposed to 20 μM MEHP.

ways such as macropinocytosis, this effect is negligible in severe deficiency (Shao et al., 2021). Placental trophoblasts, as a medium of nutrient exchange between the mother and fetus, express a large number of different types of amino acid transporters to continuously pass amino acids to the fetus (Rosario et al., 2021). Therefore, we speculate that MEHP might be responsible for the dysfunction of some amino acid transporters, which might result in abnormal levels of amino acids in trophoblasts, as demonstrated by Alfatah et al. (2019). However, our results showed that not all amino acid levels were downregulated, and some were even upregulated. This phenomenon, which leads to the accumulation of amino acids in cells, seems to be difficult to explain according to current studies, and it is possible that amino acid consumption is inhibited.

At the same time, this study also showed a significant reduction in metabolites with antioxidant effects, particularly glutathione by 92 % after 24 h of exposure to 20 μM MEHP. Previous studies have also shown that MEHP exerts adverse effects on a variety of trophoblast cells, causing substantial reactive oxygen species (ROS) accumulation in extravillous trophoblast cells, which in turn causes mitochondrial damage and apoptosis (Martinez-Razo et al., 2021). Interestingly, DEHP, the precursor of MEHP, does not cause oxidative stress in cells (Rose et al., 1999). In addition, ROS-induced mitochondrial dysfunction is bound to lead to abnormal energy-related metabolites. However, NAD^+ as an important metabolite in the energy metabolic pathway was also extremely sensitive to MEHP, with a very low EC_{+10} (0.73 μM). Petit et al. (2018) also found that MEHP exposure induced important changes in trophoblast lipids, especially in glycerolipids and glycerophospholipids. Although some changes in lipid metabolites were found in this study, the amounts were very small. This is because our untargeted metabolomics test is mainly for highly polar substances. Overall, the present study and the study by Petit J et al. are complementary, revealing the effects of MEHP on the metabolic dimension of trophoblast cells.

Recently, Bianchi et al. (2022) identified glutathione as a potential marker of MEHP exposure through proteomic analysis. However, glutathione was not the best marker in this study, and its corresponding EC_{-10} was 4.24 μM. Furthermore, an epigenome association study identified multiple DNA methylation markers exposed to MEHP; however, the sensitivity of these markers was not assessed (Lu et al., 2020). It is also uncertain how long it will change after exposure. In contrast, the MEHP exposure markers screened in this study, 5′-UMP and *N*-acetylputrescine, had lower EC_{10} than the 5th percentile concentrations of maternal peripheral blood (3.4 μM) and umbilical cord blood (2.2 μM) (Li et al., 2013). On the one hand, 5′-UMP and *N*-acetylputrescine have a high dose sensitivity, meaning that very low doses of MEHP exposure can also be monitored. On the other hand, these two markers are also time-sensitive; that is, these two-metabolite changes could be detected after 24 h of exposure.

This study has several advantages. First, this study combined general global and dose–response metabolomics methods to screen dysregulated metabolites. To the best of our knowledge, this is the first in vitro study to explore metabolite markers of MEHP exposure, and we focused primarily on MEHP exposure associated with fetal growth and development during pregnancy. In addition, this in vitro study was designed to be less heterogeneous than the in vivo study.

However, this study also has some limitations. This study was limited to in vitro experiments, and in vivo experiments and cohort validation need to be further completed in the future. Because we observed only 24 h of exposure, it can only represent acute exposure events; that is, 5′-UMP and *N*-acetylputrescine might not be applicable to chronic exposure to MEHP. This study only set up 4 groups of exposure doses. This dose resolution might be not insufficient and more likely to cause model overfitting.

5. Conclusion

In summary, this study revealed that MEHP exposure can cause metabolic disorder of trophoblasts, especially amino acids and antioxidant metabolites. The dysregulated metabolites were divided into three dose–

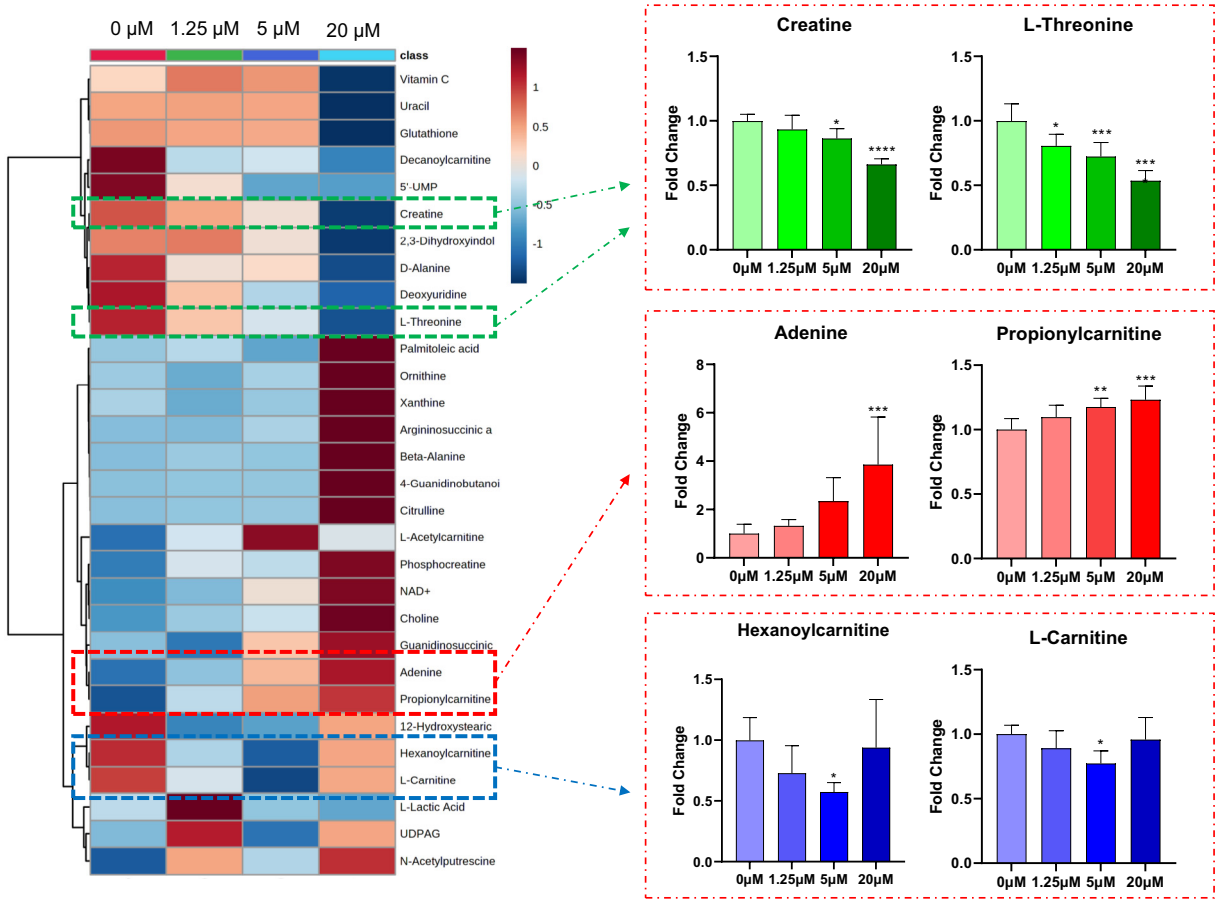

Fig. 3. Combined TOXcms dose–response metabolomics and multiple group global metabolomics for the identification of metabolites for different concentrations of MEHP. The one-way ANOVA was used to compare the metabolite FC of the three exposure groups with the control group. * <0.05, ** <0.01, *** <0.001, **** <0.0001.

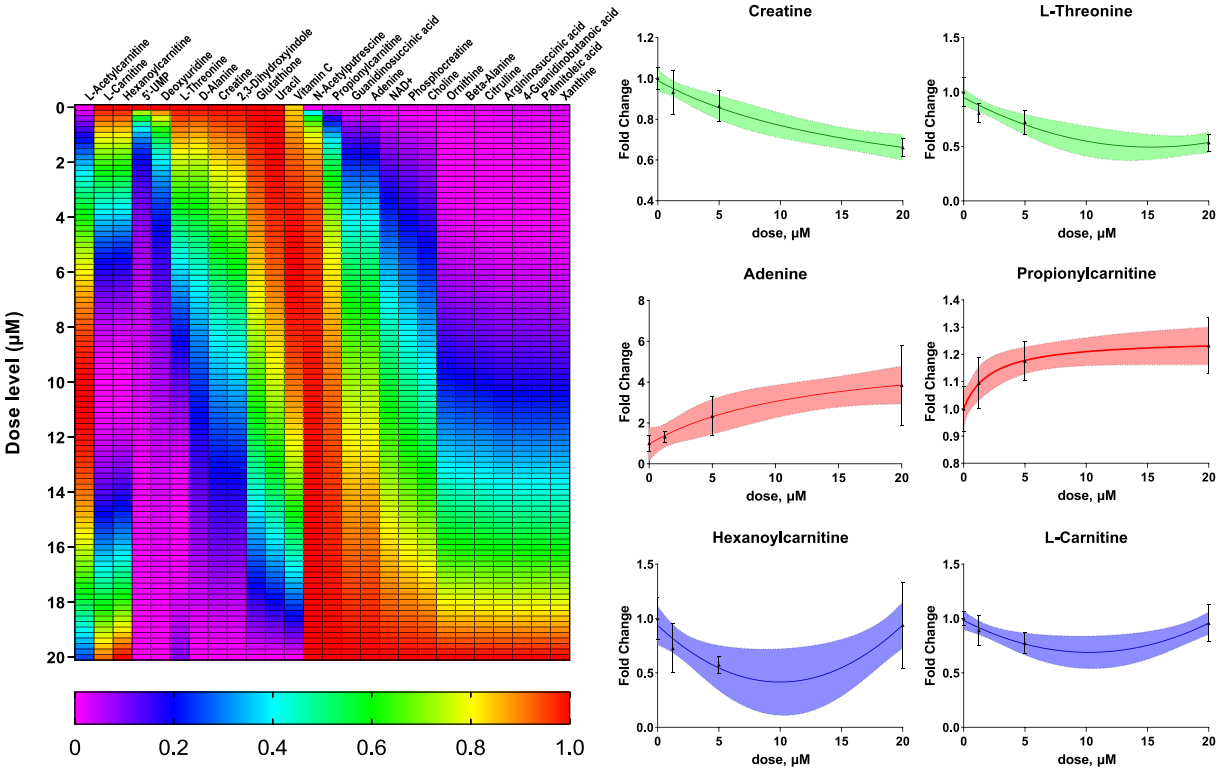

Fig. 4. Full-dose mapping of the identified metabolite models.

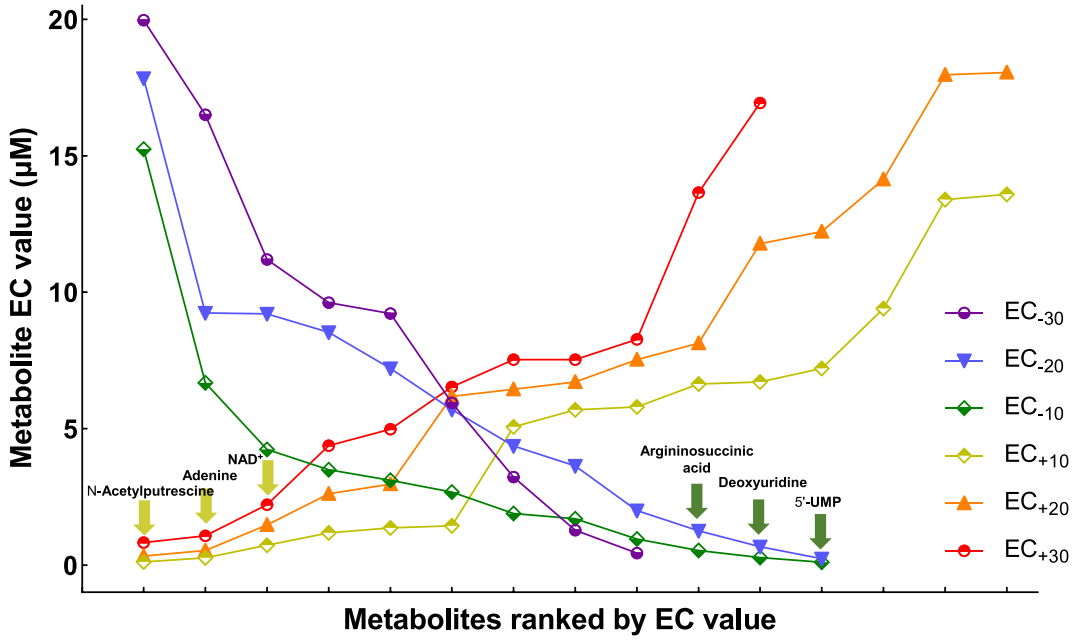

Fig. 5. Metabolite EC value ranking and perturbation biomarker screening.

response patterns: monotonic upregulation, monotonic downregulation and reversal. Most importantly, the present study identified 5′-UMP and *N*-acetylputrescine as potential markers of MEHP, providing a potential means for monitoring MEHP exposure during pregnancy.

Abbreviations

MEHP	mono(2-ethylhexyl) phthalate
PAEs	phthalic acid esters
DEHP	Di(2-ethylhexyl) phthalate
DMSO	dimethyl sulfoxide
MeOH	methanol
ACN	acetonitrile
QC	quality control
DDA	data-dependent acquisition
CD	Compound Discoverer
PCA	principal component analysis
FDR	false discovery rate
FC	fold change
ECs	effective concentrations
HMDB	Human Metabolome Database
KEGG	Kyoto Encyclopedia of Genes and Genomes
UDPAG	uridine diphosphate glucose
5′-UMP	uridine 5′-monophosphate
EC	effective concentration
ROS	reactive oxygen species
LC-MS	liquid chromatography-mass spectrometry

CRediT authorship contribution statement

Huiping Zhang and Yiwei Fang had full access to all of the data in the study and take responsibility for the integrity of the data and the accuracy of the data analysis.

Concept and design: Yiwei Fang and Huiping Zhang.

Acquisition, analysis, or interpretation of data: Yiwei Fang and Zhiliang Chen.

Drafting of the manuscript: Yiwei Fang and Jinyu Chen.

Critical revision of the manuscript for important intellectual content: Yiwei Fang, Zhiliang Chen and Jinyu Chen.

Statistical analysis: Yiwei Fang and Jinyu Chen.

Obtained funding: Huiping Zhang, Chunyan Liu, and Kai Zhao.

Administrative, technical, or material support: Minqi Zhou, Yuanyao Chen and Rong Cao.

Supervision: Huiping Zhang, Chunyan Liu, Min Wang, and Kai Zhao.

Data availability

Data will be made available on request.

Declaration of competing interest

The authors declare that they have no known competing financial interests or personal relationships that could have appeared to influence the work reported in this paper.

Acknowledgements

We are very grateful to Prof. Mingliang Fang and Dr. Haoduo Zhao (School of Civil and Environmental Engineering, Nanyang Technological University) for their help in methodology. At the same time, we are very grateful to Fan Hu (Analytical testing center-medical sub-center, Huazhong University of Science and Technology) for his vacuum centrifugal concentrator.

Funding

This work was funded by National Key Research and Development Program of China (Grant numbers: 2018YFC1004300, 2018YFC1004304).

Role of the funder/sponsor

The funding organizations had no role in the design and conduct of the study; collection, management, analysis, and interpretation of the data; preparation, review, or approval of the manuscript; and decision to submit the manuscript for publication.

Appendix A. Supplementary data

Supplementary data to this article can be found online at https://doi.org/10.1016/j.scitotenv.2022.158924.

References

Abou-Kheir, W., Barrak, J., Hadadeh, O., Daoud, G., 2017. HTR-8/SVneo cell line contains a mixed population of cells. Placenta 50, 1–7.

Aimuzi, R., Huang, S., Luo, K., Ma, S., Huo, X., Li, G., et al., 2022. Levels and health risks of urinary phthalate metabolites and the association between phthalate exposure and unexplained recurrent spontaneous abortion: a large case-control study from China. Environ. Res. 212, 113393.

Alfatah, M., Wong, J.H., Kong, K.W., Utama, F., Hoon, S., Arumugam, P., 2019. Chemical-genetic interaction landscape of mono-(2-ethylhexyl)-phthalate using chemogenomic profiling in yeast. Chemosphere 228, 219–231.

Beyer, B.A., Fang, M., Sadrian, B., Montenegro-Burke, J.R., Plaisted, W.C., Kok, B.P.C., et al., 2018. Metabolomics-based discovery of a metabolite that enhances oligodendrocyte maturation. Nat. Chem. Biol. 14, 22–28.

Bianchi, L., Casini, S., Vantaggiato, L., Di Noi, A., Carleo, A., Shaba, E., et al., 2022. A novel ex vivo approach based on proteomics and biomarkers to evaluate the effects of chrysene, MEHP, and PBDE-47 on loggerhead sea turtles (Caretta caretta). Int. J. Environ. Res. Public Health 19.

Chen, Y., Wang, H., Wang, K., Zhu, G., Yang, Z., Wang, M., et al., 2022. Serum metabolomic patterns in patients with aldosterone-producing adenoma. Front. Mol. Biosci. 9, 816469.

Chi, Z., Zhao, J., Li, W., Araghi, A., Tan, S., 2017. In vitro assessment of phthalate acid esters-trypsin complex formation. Chemosphere 185, 29–35.

Crizer, D.M., Ramaiahgari, S.C., Ferguson, S.S., Rice, J.R., Dunlap, P.E., Sipes, N.S., et al., 2021. Benchmark concentrations for untargeted metabolomics versus transcriptomics for liver injury compounds in in vitro liver models. Toxicol. Sci. 181, 175–186.

Doull, J., Cattley, R., Elcombe, C., Lake, B.G., Swenberg, J., Wilkinson, C., et al., 1999. A cancer risk assessment of di(2-ethylhexyl)phthalate: application of the new U.S. EPA Risk Assessment Guidelines. Regul. Toxicol. Pharmacol. 29, 327–357.

Elimam, M.M., Shantier, S.W., Gadkariem, E.A., Mohamed, M.A., Osman, Z., 2017. Stability studies on florfenicol using developed derivative spectrophotometric methods. Ann. Pharm. Fr. 75, 40–44.

Gani, K.M., Tyagi, V.K., Kazmi, A.A., 2017. Occurrence of phthalates in aquatic environment and their removal during wastewater treatment processes: a review. Environ. Sci. Pollut. Res. Int. 24, 17267–17284.

Gao, F., Hu, W., Li, Y., Shen, H., Hu, J., 2017. Mono-2-ethylhexyl phthalate inhibits human extravillous trophoblast invasion via the PPARgamma pathway. Toxicol. Appl. Pharmacol. 327, 23–29.

Hanioka, N., Kinashi, Y., Tanaka-Kagawa, T., Isobe, T., Jinno, H., 2017. Glucuronidation of mono(2-ethylhexyl) phthalate in humans: roles of hepatic and intestinal UDP-glucuronosyltransferases. Arch. Toxicol. 91, 689–698.

He, Y., Wang, Q., He, W., Xu, F., 2019. The occurrence, composition and partitioning of phthalate esters (PAEs) in the water-suspended particulate matter (SPM) system of Lake Chaohu,China. Sci. Total Environ. 661, 285–293.

James, J.L., Carter, A.M., Chamley, L.W., 2012. Human placentation from nidation to 5 weeks of gestation. Part I: what do we know about formative placental development following implantation? Placenta 33, 327–334.

Li, L.X., Chen, L., Meng, X.Z., Chen, B.H., Chen, S.Q., Zhao, Y., et al., 2013. Exposure levels of environmental endocrine disruptors in mother-newborn pairs in China and their placental transfer characteristics. PLoS One 8, e62526.

Li, X.N., Li, H.X., Yang, T.N., Li, X.W., Huang, Y.Q., Zhu, S.Y., et al., 2020. Di-(2-ethylhexyl) phthalate induced developmental abnormalities of the ovary in quail (Coturnix japonica) via disruption of the hypothalamic-pituitary-ovarian axis. Sci. Total Environ. 741, 140293.

Liang, D., Moutinho, J.L., Golan, R., Yu, T., Ladva, C.N., Niedzwiecki, M., et al., 2018. Use of high-resolution metabolomics for the identification of metabolic signals associated with traffic-related air pollution. Environ. Int. 120, 145–154.

Liu, S., Yang, R., Yang, Q., He, G., Chen, B., Dong, R., 2022. The independent and interactive effects of phthalates exposure and hypertension on the indicators of early renal injury in US adults: evidence from NHANES 2001–2004. Environ. Res. 213, 113733.

Lu, X., Fraszczyk, E., van der Meer, T.P., van Faassen, M., Bloks, V.W., Kema, I.P., et al., 2020. An epigenome-wide association study identifies multiple DNA methylation markers of exposure to endocrine disruptors. Environ. Int. 144, 106016.

Martinez-Razo, L.D., Martinez-Ibarra, A., Vazquez-Martinez, E.R., Cerbon, M., 2021. The impact of di-(2-ethylhexyl) phthalate and mono(2-ethylhexyl) phthalate in placental development, function, and pathophysiology. Environ. Int. 146, 106228.

Midic, U., Goheen, B., Vincent, K.A., VandeVoort, C.A., Latham, K.E., 2018. Changes in gene expression following long-term in vitro exposure of Macaca mulatta trophoblast stem cells to biologically relevant levels of endocrine disruptors. Reprod. Toxicol. 77, 154–165.

Minguez-Alarcon, L., Williams, P.L., James-Todd, T., Souter, I., Ford, J.B., Rexrode, K.M., et al., 2022. Association of urinary phthalate and phthalate replacement metabolite concentrations with serum lipid biomarker levels among pregnant women attending a fertility center. Toxics 10.

Pang, Z., Chong, J., Zhou, G., de Lima Morais, D.A., Chang, L., Barrette, M., et al., 2021. MetaboAnalyst 5.0: narrowing the gap between raw spectra and functional insights. Nucleic Acids Res. 49, W388–W396.

Perez-Albaladejo, E., Fernandes, D., Lacorte, S., Porte, C., 2017. Comparative toxicity, oxidative stress and endocrine disruption potential of plasticizers in JEG-3 human placental cells. Toxicol. in Vitro 38, 41–48.

Petit, J., Wakx, A., Gil, S., Fournier, T., Auzeil, N., Rat, P., et al., 2018. Lipidome-wide disturbances of human placental JEG-3cells by the presence of MEHP. Biochimie 149, 1–8.

Pollheimer, J., Vondra, S., Baltayeva, J., Beristain, A.G., Knofler, M., 2018. Regulation of placental extravillous trophoblasts by the maternal uterine environment. Front. Immunol. 9, 2597.

Rosario, F.J., Kramer, A., Li, C., Galan, H.L., Powell, T.L., Nathanielsz, P.W., et al., 2021. Reduction of in vivo placental amino acid transport precedes the development of intrauterine growth restriction in the non-human primate. Nutrients 13.

Rose, M.L., Rivera, C.A., Bradford, B.U., Graves, L.M., Cattley, R.C., Schoonhoven, R., et al., 1999. Kupffer cell oxidant production is central to the mechanism of peroxisome proliferators. Carcinogenesis 20, 27–33.

Sardon, H., Dove, A.P., 2018. Plastics recycling with a difference. Science 360, 380–381.

Shao, X., Cao, G., Chen, D., Liu, J., Yu, B., Liu, M., et al., 2021. Placental trophoblast syncytialization potentiates macropinocytosis via mTOR signaling to adapt to reduced amino acid supply. Proc. Natl. Acad. Sci. U. S. A. 118.

Shen, X., Wang, C., Liang, N., Liu, Z., Li, X., Zhu, Z.-J., et al., 2021. Serum metabolomics identifies dysregulated pathways and potential metabolic biomarkers for hyperuricemia and gout. Arthritis Rheumatol. 73, 1738–1748.

Wei, X., Yang, D., Zhang, B., Fan, X., Du, H., Zhu, R., et al., 2022. Di-(2-ethylhexyl) phthalate increases plasma glucose and induces lipid metabolic disorders via FoxO1 in adult mice. Sci. Total Environ. 156815.

Xu, Y., Cook, T.J., Knipp, G.T., 2005. Effects of di-(2-ethylhexyl)-phthalate (DEHP) and its metabolites on fatty acid homeostasis regulating proteins in rat placental HRP-1 trophoblast cells. Toxicol. Sci. 84, 287–300.

Xu, Y., Knipp, G.T., Cook, T.J., 2006. Effects of di-(2-ethylhexyl)-phthalate and its metabolites on the lipid profiling in rat HRP-1 trophoblast cells. Arch. Toxicol. 80, 293–298.

Xu, M., Li, Y., Wang, X., Zhang, Q., Wang, L., Zhang, X., et al., 2022. Role of hepatocyte- and macrophage-specific PPARgamma in hepatotoxicity induced by diethylhexyl phthalate in mice. Environ. Health Perspect. 130, 17005.

Yao, C.H., Wang, L., Stancliffe, E., Sindelar, M., Cho, K., Yin, W., et al., 2020. Dose-response metabolomics to understand biochemical mechanisms and off-target drug effects with the TOXcms software. Anal. Chem. 92, 1856–1864.

Zhang, S., Sun, C., Zhao, S., Wang, B., Wang, H., Zhang, J., et al., 2020a. Exposure to DEHP or its metabolite MEHP promotes progesterone secretion and inhibits proliferation in mouse placenta or JEG-3 cells. Environ. Pollut. 257, 113593.

Zhang, T.D., Ma, Y.B., Li, H.C., Chong, T., Wang, Z.M., Zhang, L.D., 2020b. Low dose of genistein alleviates mono-(2-ethylhexyl) phthalate-induced fetal testis disorder based on organ culture model. Oxidative Med. Cell. Longev. 2020, 4569268.

Zhao, H., Liu, M., Lv, Y., Fang, M., 2022. Dose-response metabolomics and pathway sensitivity to map molecular cartography of bisphenol A exposure. Environ. Int. 158, 106893.